Reprinted from
IEEE Microwave and Wireless Components Letters, Vol. 15, No. 11, January 2005

Coupling Behaviors of Quarter-Wavelength Impedance Transformers for Wideband CPW Bandpass Filters

Lei Zhu, *Senior Member, IEEE*, Huamin Shi, and Wolfgang Menzel, *Fellow, IEEE*

***Abstract*—Quarter-wavelength coplanar waveguide ($\lambda/4$-CPW) impedance transformers with low and high characteristic impedance are characterized via fullwave method of moments short-open calibration (MoM-SOC) approach and further utilized as alternative K- and J-inverter networks with enhanced coupling. Network parameters are obtained and compared with those of two traditional lumped-CPW elements, demonstrating tightened coupling behaviors. The two improved $\lambda/4$ CPW bandpass filters are then constructed and their performances are optimized via cascaded topology. Predicted results show us a few attractive features, i.e., wide passband and first-order harmonic suppression as confirmed by experiment.**

***Index Terms*—Coplanar waveguide (CPW) coupling structures, harmonic suppression, $\lambda/4$ CPW bandpass filter, $\lambda/4$ impedance transformer, wide passband.**

I. INTRODUCTION

COPLANAR waveguide (CPW) bandpass filters with size-compactness have been attracting a rapidly increasing interest in the exploration of high-frequency integrated circuits. In [1], a capacitively end-coupled CPW bandpass filter was initially proposed by cutting gaps in the central conductor of CPW. To circumvent the problem of high radiation loss happened around the gaps, an alternative inductively end-coupled bandpass filter was developed by electrically connecting the inner and outer conductors together via metallic strip with narrow widths [2]. It needs to be pointed out here that the two above filter blocks are built up on a basis of half-wavelength ($\lambda/2$) CPW resonators. In order to reduce the whole dimension, the $\lambda/4$ CPW resonator is recently utilized in the filter design. In this way, its two ends are driven by series-capacitive and shunt-inductive coupling elements [3], [4], respectively, thereby removing out the first-order harmonic in conjunction with the $\lambda/2$ resonance.

In order to design the CPW filters with relatively wide bandwidth, one usually finds out that the coupling degree of two traditional lumped coupling elements, as illustrated in Figs. 1(a) and 2(a), is not sufficiently large especially at low frequency range, under the limitation of fabrication tolerance. To effectively address this issue, several parallel-coupled CPW coupling structures driven with two asymmetrical CPW feeding lines were proposed [5]. In this work, the two simple $\lambda/4$ impedance transformers with low and high characteristic impedances are studied with the configurations as shown in Figs. 1(b) and 2(b), and they are then utilized as alternative K- and J-inverters for design of $\lambda/4$ CPW bandpass filter with widened bandwidth. After their coupling behaviors are comparatively studied via fullwave method of moments short-open calibration (MoM-SOC) technique [6], [7], the improved second- and fourth-order $\lambda/4$ CPW bandpass filters are designed and predicted results are then supported by experiment over a wide frequency range.

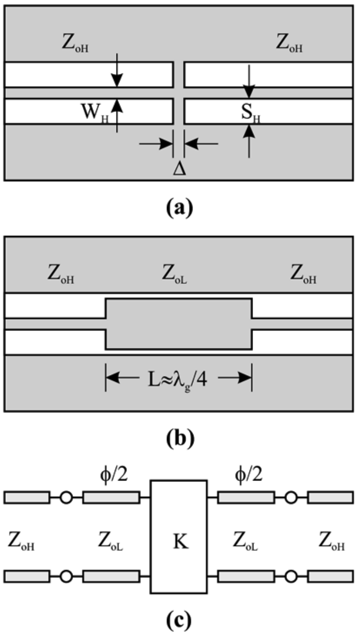

Fig. 1. Schematics and equivalent K-inverter networks of traditional and proposed CPW inductive coupling structures. (a) Lumped-K. (b) $\lambda/4$-transformer. (c) Equivalent network.

II. COUPLING STRUCTURES: $\lambda/4$ CPW TRANSFORMERS

Figs. 1(b) and 2(b) depict the schematics of $\lambda/4$ CPW impedance transformers with low and high characteristic impedances as compared with their CPW feeding line counterparts, respectively. Using the approach as detailed in [6]–[8], the relevant two-port Z- or Y-matrix parameters can be de-embedded at the references of two step interfaces. Thus, characteristic impedances of various uniform CPW impedance transformers can be numerically derived [7].

Manuscript received January 29, 2004; revised July 14, 2004. The review of this letter was arranged by Associate Editor A. Weisshaar.

L. Zhu and H. Shi are with the School of Electrical and Electronic Engineering, Nanyang Technological University, Singapore 639798 (e-mail: ezhul@ntu.edu.sg).

W. Menzel is with the Department of Microwave Techniques, University of Ulm, Ulm D-89069, Germany.

Digital Object Identifier 10.1109/LMWC.2004.840956

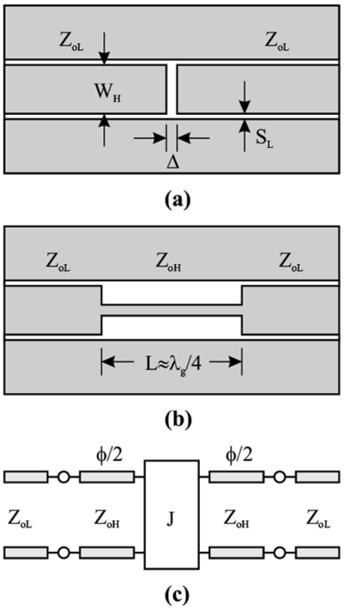

Fig. 2. Schematics and equivalent J-inverter networks of traditional and proposed CPW capacitive coupling structures. (a) Lumped-J. (b) $\lambda/4$-transformer. (c) Equivalent network.

Fig. 1(c) denotes the equivalent K-inverter network of the shunt-inductive coupling structures in Fig. 1(a) and (b). Meanwhile, Fig. 2(c) is the equivalent J-inverter network of series-capacitive coupling structures in Fig. 2(a) and (b). Their parameters, including K-inverter impedance (K) and J-inverter admittance (J), can be derived in terms of two sets of closed-form equations under the equivalence of two networks for the same physical layout.

For instances, the normalized K-impedance and J-admittance, i.e., $\bar{K}$ and $\bar{J}$, can be explicitly expressed in terms of the normalized characteristic admittances and impedances, $\bar{Y}_{\rm oL}, \bar{Z}_{\rm oL}, \bar{Y}_{\rm oH}$, and $\bar{Z}_{\rm oH}$, with resorting to those of their two CPW feeding lines¼

$$\bar{K} = -\frac{\sin\theta}{2}\left[\left(\bar{Z}_{\rm oL} - \bar{Y}_{\rm oL}\right) + \frac{\bar{Z}_{\rm oL} + \bar{Y}_{\rm oL}}{\cos\phi}\right] \qquad (1)$$

$$\bar{J} = -\frac{\sin\theta}{2}\left[\left(\bar{Y}_{\rm oH} - \bar{Z}_{\rm oH}\right) + \frac{\bar{Y}_{\rm oH} + \bar{Z}_{\rm oH}}{\cos\phi}\right] \qquad (2)$$

where θ denotes the electrical length or phase of the CPW transformers with the length (L) while ϕ denotes the equivalent phase at the two sides of J- or K-inverter.

Let's at first consider the CPW K- and J-inverter structures with the fixed 50 Ω feeding lines fabricated on the RT/Duroid 6010 with the permittivity of $\varepsilon_{\rm r} = 10.8$ and thickness of $h = 0.635$ mm. Fig. 3(a) depicts the normalized K-impedance of the $\lambda/4$ impedance transformer with low impedance $(Z_{\rm oL})$ as in Fig. 1(b). As the slot width $(S_{\rm L})$ is reduced from 0.570 mm (50 Ω case) to 0.127 mm, $|K/Z_{\rm oH}|$ with solid line is observed to gradually fall down around the frequency range of $\lambda/4$. In the meantime, $|K/Z_{\rm oH}|$ of lumped-K element in Fig. 1(a) seems linear increment with the frequency and the relevant slope or coupling degree gets slight enlarged as the gap width Δ decreases. By comparing these two sets of graphs, the proposed transformer-based K-inverter is seen to have much high coupling strength rather than its traditional counterpart.

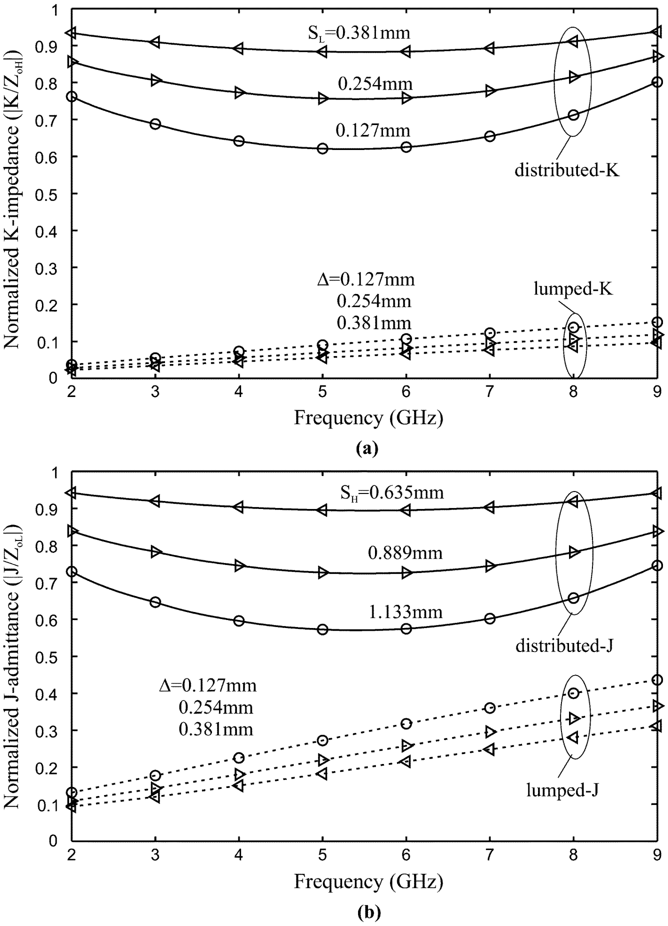

Fig. 3. Normalized K-impedance and J-admittance versus frequency for comparative investigation. (a) K-inverter structures. (b) J-inverter structures.

Fig. 3(b) illustrates the two sets of normalized J-inverter structures in Fig. 2(b) and (a). By widening the slot width $(S_{\rm L})$ in the CPW transformer, the normalized $|J/Y_{\rm oL}|$ is again observed to fall down below the unity value around the frequency range of $\lambda/4$. In parallel, $|J/Y_{\rm oL}|$ of the traditional one goes up as the frequency increases and the gap width Δ decreases, but its coupling quantity is still very smaller than that of the proposed one.

III. IMPROVED $\lambda/4$ CPW BANDPASS FILTERS

Based on the above-discussed coupling behaviors, the two CPW impedance transformers are used as an enhanced K- or J-inverter for design of $\lambda/4$ CPW filters [3], [4] with relatively wide bandwidth. Fig. 4(a) is the layout of the second-order $\lambda/4$ CPW bandpass filter. Herein, the $\lambda/4$ transformer with low impedance is constructed and put at both input and output in order to effectively use its high K-impedance as derived in Fig. 3(a). Furthermore, the two $\lambda/4$ CPW resonators are linked together via series capacitive gap coupling element with small J-admittance as in Fig. 3(b).

As discussed in [8], each CPW step discontinuity can be modeled as a single shunt capacitance while the uniform CPW section with different transversal dimensions can be modeled in terms of their characteristic impedances and effective dielectric constants. Thus, a unified equivalent cascaded network can be formulated to implement the optimization design of the whole

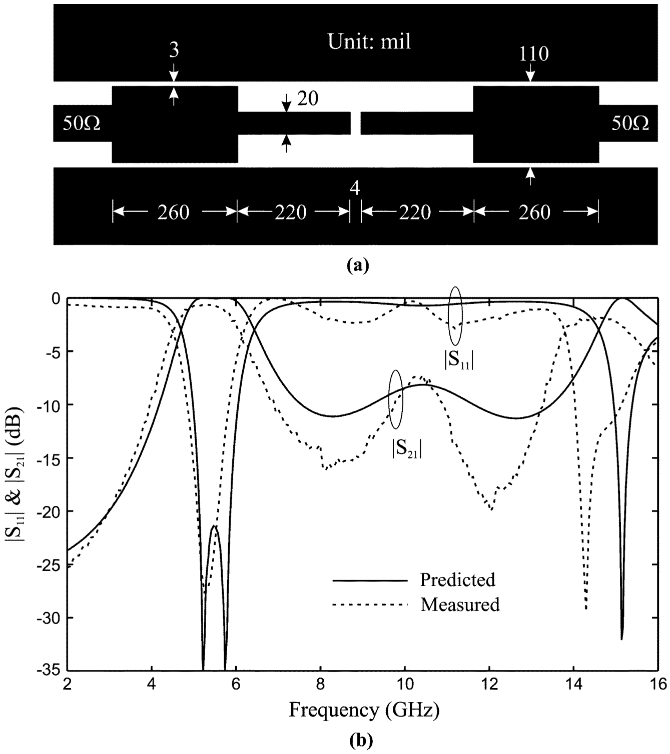

Fig. 4. Layout and predicted/measured results of a second-order $\lambda/4$ CPW bandpass filter. (a) Layout. (b) Predicted and measured results.

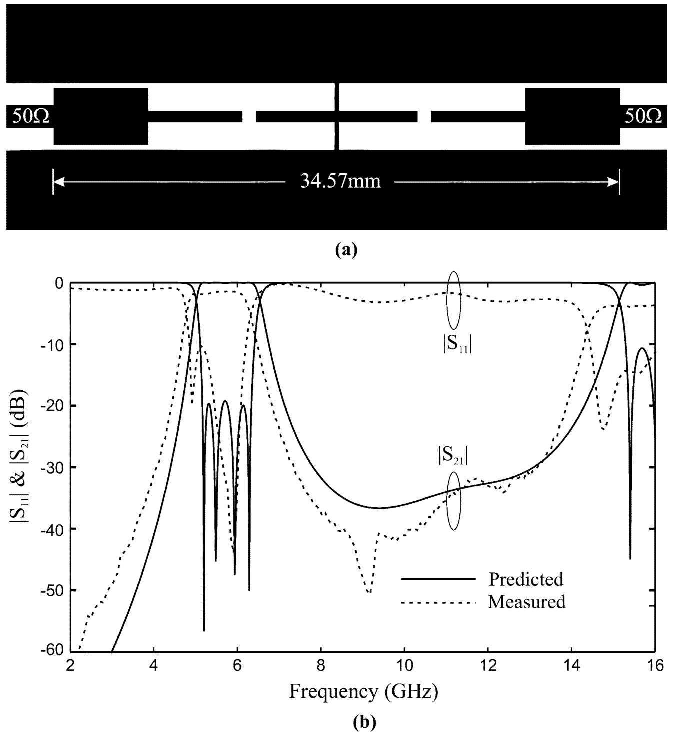

Fig. 5. Layout and predicted/measured results of a fourth-order $\lambda/4$ CPW bandpass filter. (a) Layout. (b) Predicted and measured results.

filter block on a basis of a simple cascaded network. Fig. 4(b) illustrates the two sets of S-parameters in a wide frequency range. Our network-predicted results exhibit us a few attractive performances of this filter, e.g., widened passband of about 28% at the central frequency of 5.5 GHz and complete suppression of the first-order harmonic around 11.0 GHz. Measured results are observed in reasonable agreement with predicted ones over the range and some visible discrepancies among them may be primarily caused by theoretically approximate characterization of metallic thickness especially around CPW transformer.

In order to achieve the better bandpass behavior with higher rejection outside the passband, a fourth-order $\lambda/4$ CPW bandpass filter, as shown in Fig. 5(a), is further designed. Based on the different quantities of coupling degree as illustrated in Fig. 3(a) and (b), the series-inductively end-coupled element is arranged at the center considering its weak K-impedance while the CPW impedance transformers and capacitive gap-coupling elements are still used as before. Network-based optimization is carried out toward the return loss $(|S_{11}|)$ less than -20 dB within the passband. Fig. 5(b) shows the predicted S-parameters together with the measured ones. Predicted results clearly exhibit us the four transmission poles within the passband. Moreover, both the two sets of graphs demonstrate that the upper stopband with the range of 7.0 to 15.0 GHz is significantly lowered while the bandpass behavior gets a great improvement with very steep rejection outside the passband.

IV. CONCLUSION

In this work, the $\lambda/4$ impedance transformer with low or high characteristic impedance is modeled and then utilized as enhanced K- or J-inverter for filter design. Comparative investigation on the lumped-element and transformer-based coupling structures are implemented in terms of normalized K- or J-inverter parameters. Derived results indicate us that the $\lambda/4$ impedance transformer can achieve highly enhanced inductive or capacitive coupling degree. Afterwards, the second- and fourth-order $\lambda/4$ CPW bandpass filters are designed with the widened passband of about 25–30% and they are realized via enhanced K-impedance of a $\lambda/4$ CPW transformer with lower characteristic impedance. Relevant predicted results are then confirmed by our experiment over a wide frequency range.

REFERENCES

[1] D. F. Williams and S. E. Schwarz, "Design and performance of coplanar waveguide bandpass filters," *IEEE Trans. Microw. Theory Tech.*, vol. 31, no. 7, pp. 558–566, Jul. 1983.

[2] J. K. A. Everard and K. K. M. Cheng, "High performance direct coupled bandpass filters on coplanar waveguide," *IEEE Trans. Microw. Theory Tech.*, vol. 41, no. 9, pp. 1568–1573, Sep. 1993.

[3] T. Tsujiguchi, H. Matsumoto, and T. Nishikawa, "A miniaturized end-coupled bandpass filter using $\lambda/4$ hair-pin coplanar resonators," in *IEEE MTT-S Int. Dig.*, Jun. 1998, pp. 829–832.

[4] A. Sanada, H. Takehara, and I. Awai, "Design of the CPW in-line $\lambda/4$ stepped-impedance resonator bandpass filter," in *Proc. Asia-Pacific Microwave Conf. Proc.*, Dec. 2001, pp. 633–636.

[5] W. Menzel, W. Schwab, and G. Grauss, "Investigation of coupling structures for coplanar bandpass filters," in *IEEE MTT-S Int. Dig.*, Jun. 1995, pp. 1407–1410.

[6] L. Zhu and K. Wu, "Short-open calibration technique for field theory-based parameter extraction of lumped-elements of planar integrated circuits," *IEEE Trans Microw. Theory Tech.*, vol. 50, no. 8, pp. 1861–1869, Aug. 2002.

[7] L. Zhu, "Unified 3-D definition of CPW- and CSL-mode characteristic impedances of coplanar waveguide using MoM-SOC technique," *IEEE Microw. Wireless Compon. Lett.*, vol. 13, no. 4, pp. 158–160, Apr. 2003.

[8] L. Zhu and T. Yakabe, "Fullwave MoM-SOC technique for extraction of equivalent circuit models coplanar waveguide discontinuities: CPW- and CSL-mode cases," *IEICE Trans. Electron.*, vol. E86-C, no. 11, pp. 2292–2299, Nov. 2003.